Heat Conduction Analysis in Bodies Containing Thin-Walled Structures by Means of Hybrid BNM with an Application to CNT-Based Composites*

Jianming ZHANG**, Masataka TANAKA***, Toshiro MATSUMOTO**** and Artur GUZIK†

This paper discusses an implementation of Hybrid Boundary Node Method (Hybrid BNM) to the heat conduction analysis within bodies containing thin-walled structures. As an application, the thermal analysis in carbon nanotubes (CNT) based composites is presented. CNTs are predicted to possess superior heat conductivity and may, even with a small amount embedded, substantially improve heat conducting behavior of polymers. In this paper the equivalent heat conductivities of CNT-based nanocomposites are evaluated using a 3-D nanoscale representative volume element (RVE) model and the hybrid boundary node method (Hybrid BNM). The temperature distribution and heat flux concentration are studied. The equivalent heat conductivity of the RVE as a function of the nanotube length is calculated and discussed, and, moreover, an approximate formula for its evaluation for an RVE containing single nanotube is proposed. Computations indicate that addition of about 7.2% to 17% (volume fraction) of CNT to the polymer matrix may result in the increase of heat conductivity of the composite varying from 49% to 334% both for short and long CNT.

Key Words: Carbon Nanotube, Nanocomposites, Heat Conductivity, Hybrid Boundary Node Method

1. Introduction

Over the last decade carbon nanotubes (CNT) have been attracting considerable attention from both scientists and engineers. Due to their near-perfect nanostructure, which can be thought of as a hexagonal sheet of carbon atoms rolled into a seamless cylinder with two semisphere caps at each end, the carbon nanotubes are predicted to possess exceptional physical properties such as superior heat and electrical conductivities, as well as high stiffness, strength and resilience.

Intensive research has been carried out on these quasi-one-dimensional structures concerning their production, physical properties and possible applications[1),(2)]. A few recent experiments have been reported on mats of compressed ropes of CNTs[3),(4)]. By assuming that both thermal and electrical conductivities follow the same rules for transport, values of thermal conductivity of CNTs, ranging from 1 750 to 5 850 W/m·K, have been extrapolated from experimental measurement on mats of nanotube ropes. The direct measurements of individual nanotube were also performed using MEMS measurement technology[5)]. Following those experiments, several preliminary molecular dynamics simulations[6)–(8)] of the thermal conductivity gave even higher values, namely, 6 600 W/m·K at 300 K[6)]. Although the estimated values of thermal conductivity were different from each other, it is generally accepted that the CNTs possess excellent heat conductivity, comparable or even higher than diamond, considered so far as the best heat conductor. Unlike the electrical conductivity, no significant dependence on the nanotube chirality is seen, while its strong dependence on radius[7)]. Moreover, the heat conductivity of a CNT is less sensitive to the defects and voids than that of diamond[8)].

These remarkable properties may make CNTs ideal

* Received 6th May, 2003 (No. 03-4051)

** Faculty of Engineering, Shinshu University, Nagano 380–8553, Japan. E-mail: zhangjm@homer.shinshu-u.ac.jp

*** Faculty of Engineering, Shinshu University, Nagano 380–8553, Japan. E-mail: dtanaka@gipwc.shinshu-u.ac.jp

**** Faculty of Engineering, Shinshu University, Nagano 380–8553, Japan. E-mail: toshiro@gipwc.shinshu-u.ac.jp

† Faculty of Engineering, Shinshu University, Nagano 380–8553, Japan. E-mail: guzik@homer.shinshu-u.ac.jp, on leave from CUT, Cracow, Poland

for a wide range of technological applications. One of the most intriguing applications is the use of CNTs, as a small volume fraction filler, in nanotube-reinforced polymers. CNT-based composites offer significant improvements to structural properties over their base polymers. It has been demonstrated that with only 1% (weight fraction) of CNTs added to a matrix material, the stiffness of a resulting composite can increase as high as 36 – 42% and the tensile strength up to 25%[9]. Most of numerical simulations so far have been focused on characterizing the effective mechanical properties of the nanocomposites, such as Young's modulus[10),(11)], while relatively fewer studied the thermal conductivities. The thermal properties of the CNT-based composites are as important as their mechanical properties in engineering applications.

The main aim of this study is to gain insight into the thermal properties of CNT-based composites through numerical simulation based on continuum approach. The equivalent heat conductivity of carbon nanotube-based composites is evaluated using a representative volume element (RVE) based on 3-D potential theory and solved by means of the hybrid boundary node method combined with a multi-domain solver. The temperature distribution and flux concentration in an RVE containing single nanotube are investigated.

2. Computational Techniques and Models

Numerical simulations can play an important role in the development of the CNT-based composites and help to understand the physical phenomena and, furthermore, analysis and design of such nanocomposites. At the nanoscale level, tests are both extremely difficult and expensive to perform. Modeling and simulations, on the other hand, can be readily achieved and are cost effective. Characterizing the physical properties of CNT-based composites is just one of the many important and urgent tasks that simulations can accomplish.

Simulations of individual CNTs using atomistic or molecular dynamics (MD) models have provided abundant results helping in understanding their thermal, mechanical and electrical behaviors. However, these simulations are so far limited to very small length and time scales and cannot deal with the larger models, mainly due to the limitations in current computing power. Continuum mechanics has also been successfully applied for individual CNTs or CNT bundles to investigate their mechanical properties. Although the validity of the continuum approach to modeling of CNTs is still not fully confirmed and will continue to be questioned, it seems at present to be the only feasible approach for carrying some preliminary simulations of CNT-based composites.

One of the methods of developing manageable 3-D continuum models for the study of CNT-based composites is to extend the concept of representative volume element used for conventional fiber-reinforced composites at the microscale[12]. In the RVE approach, a single/multiple nanotube(s) with surrounding matrix material are modeled, with properly applied boundary and interface conditions to account for the effects of the surrounding materials. Liu et al.[10] applied the FEM to analyze the mechanical responses of these RVEs with single nanotube included under different loading conditions, and estimated the material constants of the nanocomposites. Fisher et al.[11] analyzed the effects of the nanotube waviness on the modulus of the nanocomposites using a RVE with a curved nanotube.

CNTs are different in size and form when they are dispersed in a matrix to make a nanocomposites. They can be single- or multi-walled with lengths varying from a few nanometers to micrometers, and might be straight, twisted and curled or in the form of ropes. Their distribution and orientation in the matrix can be uniform, unidirectional or random. All of these factors make the numerical simulations of CNT-based composites extremely difficult.

The most critical part of any numerical analysis is the discretization of domain of interest. If the domain contains thin-walled structures of complex geometry (e.g. twisted, curved, randomly distributed), the task of its proper/high quality meshing is always challenging. An implementation of Finite Element Method (FEM) to the modeling of such types of structures results in extremely large number of elements, due to obvious restriction of element connectivity and requirements of appropriate values of their aspect ratios. The Boundary Element Method (BEM) based models partially alleviate the problem, as the discretization of boundary surfaces (instead of volumes) is required, only. However, still in many cases the high quality boundary elements may be difficult and cumbersome to obtain. To overcome meshing problems, we developed the Hybrid Boundary Node Method (Hybrid BNM)[13)–(17)]. By combining a modified functional with the moving least squares (MLS) approximation, the Hybrid BNM is a truly meshless, boundary-only method. The Hybrid BNM requires only the discrete nodes located on the surface of the domain (for details, refer to Ref.(17)) and, hence, considerably simplifies the discretization task. Moreover, it uses the parametric representation of domain surfaces, only. Such representation is used in any CAD software and can be accessed in commercial packages via *Open Architecture* features (usually the in-process COM servers/objects can be exploited). This may considerably simplify the data pre-processing and discretization tasks and lead to substantial resources savings.

In the next section, the Hybrid BNM is incorporated into a multi-domain solver to compute the RVE with single nanotube inserted. To our best knowledge, it is the first attempt to evaluate thermal properties of nanocomposites using the RVE approach.

3. Hybrid BNM for Multi-Domain Models

For the sake of simplicity, only, two domains, i.e. the nanotube and the polymer are considered here. It is assumed that both the CNT and matrix in the RVE are continua of linear, isotropic and homogenous materials with given heat conductivities. A steady state heat conduction problem governed by Laplace's equation with proper boundary conditions is considered for each domain.

The hybrid boundary node method is based on a modified variational principle, in which there are three independent variables, namely:

— temperature within the domain, ϕ;

— boundary temperature, $\tilde{\phi}$;

— boundary normal heat flux, $\tilde{q}$.

Suppose that N nodes are randomly distributed on the bounding surface of a single domain. The domain temperature is approximated using fundamental solutions as follows:

$$\phi = \sum_{I=1}^{N} \phi_I^s x_I, \tag{1}$$

and hence at a boundary point, the normal heat flux is given by:

$$q = -\kappa \sum_{I=1}^{N} \frac{\partial \phi_I^s}{\partial n} x_I, \tag{2}$$

where ϕ_I^s is the fundamental solution with the source at a node $\boldsymbol{s}_I$, κ is the heat conductivity and x_I are unknown parameters. For 3-D steady state heat conduction problems, the fundamental solution can be written as

$$\phi_I^s = \frac{1}{\kappa} \frac{1}{4\pi r(Q, \boldsymbol{s}_I)}, \tag{3}$$

where Q is a field point; $r(Q, \boldsymbol{s}_I)$ is the distance between the point Q and the node $\boldsymbol{s}_I$.

The boundary temperature and normal heat flux are interpolated by moving least square (MLS) approximation:

$$\tilde{\phi}(\boldsymbol{s}) = \sum_{I=1}^{N} \Phi_I(\boldsymbol{s}) \hat{\phi}_I, \tag{4}$$

and

$$\tilde{q}(\boldsymbol{s}) = \sum_{I=1}^{N} \Phi_I(\boldsymbol{s}) \hat{q}_I. \tag{5}$$

In the foregoing equations, $\Phi_I(\boldsymbol{s})$ is the shape function of MLS approximation; $\hat{\phi}_I$ and $\hat{q}_I$ are nodal values of temperature and normal flux, respectively.

For the polymer domain, the following set of equations, expressed in matrix form, is given:

$$\begin{bmatrix} U_{00}^p & U_{01}^p \\ U_{10}^p & U_{11}^p \end{bmatrix} \begin{Bmatrix} x_0^p \\ x_1^p \end{Bmatrix} = \begin{Bmatrix} H_0^p \hat{\phi}_0^p \\ H_1^p \hat{\phi}_1^p \end{Bmatrix}, \tag{6}$$

$$\begin{bmatrix} V_{00}^p & V_{01}^p \\ V_{10}^p & V_{11}^p \end{bmatrix} \begin{Bmatrix} x_0^p \\ x_1^p \end{Bmatrix} = \begin{Bmatrix} H_0^p \hat{q}_0^p \\ H_1^p \hat{q}_1^p \end{Bmatrix}, \tag{7}$$

where superscripts/subscript p, 0 and 1 stand for polymer, quantities exclusively associated with a domain, and quantities associated with the interface, respectively. The submatrices $[U]$, $[V]$ and $[H]$ are defined as:

$$U_{IJ} = \int_{\Gamma_s^J} \phi_I^s v_J(Q) d\Gamma, \tag{8}$$

$$V_{IJ} = \int_{\Gamma_s^J} q_I^s v_J(Q) d\Gamma, \tag{9}$$

$$H_{IJ} = \int_{\Gamma_s^J} \Phi_I(\boldsymbol{s}) v_J(Q) d\Gamma, \tag{10}$$

where Γ_s^J is a regularly shaped local region around a given node $\boldsymbol{s}_J$, v_J is a weight function and $\boldsymbol{s}$ is a boundary point.

Similarly, for the nanotube domain we have:

$$\begin{bmatrix} U_{00}^n & U_{01}^n \\ U_{10}^n & U_{11}^n \end{bmatrix} \begin{Bmatrix} x_0^n \\ x_1^n \end{Bmatrix} = \begin{Bmatrix} H_0^n \hat{\phi}_0^n \\ H_1^n \hat{\phi}_1^n \end{Bmatrix}, \tag{11}$$

and

$$\begin{bmatrix} V_{00}^n & V_{01}^n \\ V_{10}^n & V_{11}^n \end{bmatrix} \begin{Bmatrix} x_0^n \\ x_1^n \end{Bmatrix} = \begin{Bmatrix} H_0^n \hat{q}_0^n \\ H_1^n \hat{q}_1^n \end{Bmatrix}, \tag{12}$$

where the superscript n stands for the nanotube.

As the continuity and equilibrium conditions at the interface between the nanotube and the polymer must be satisfied, i.e.:

$$\{\phi_1^p\} = \{\phi_1^n\} \tag{13}$$

and

$$\{q_1^p\} = -\{q_1^n\}, \tag{14}$$

Eqs. (6), (7), (11) and (12) can be assembled into the following expression:

$$\begin{bmatrix} A_{00}^p & A_{01}^p & 0 & 0 \\ U_{10}^p & U_{11}^p & -U_{10}^n & -U_{11}^n \\ V_{10}^p & V_{11}^p & V_{10}^n & V_{11}^n \\ 0 & 0 & A_{00}^n & A_{01}^n \end{bmatrix} \begin{Bmatrix} x_0^p \\ x_1^p \\ x_0^n \\ x_1^n \end{Bmatrix} = \begin{Bmatrix} H_0^p d_0^p \\ 0 \\ 0 \\ H_0^n d_0^n \end{Bmatrix}, \tag{15}$$

where $[A_{0i}^*]$ and $\{d_i^*\}$ ($*$ represents p or n; i indicates 0 or 1) are formed by merging $[U_{0i}^*]$ and $[V_{0i}^*]$, $\{\hat{\phi}_0^*\}$ and $\{\hat{q}_0^*\}$ according the known boundary conditions, respectively. For degrees of freedom with prescribed temperature, the related elements in $\{\hat{\phi}_0^*\}$ are selected for $\{d_i^*\}$, and the corresponding rows of in $[U_{0i}^*]$ are selected for $[A_{0i}^*]$; otherwise, elements in $\{\hat{q}_0^*\}$ are selected for $\{d_i^*\}$, and the corresponding rows in $[V_{0i}^*]$ are selected for $[A_{0i}^*]$.

The set of Eq. (15) is solved for unknown parameters $\boldsymbol{x}$, and then, by back-substitution into Eqs. (6), (7), (11) and (12), the boundary unknowns are obtained either on the interface or the external boundary.

As demonstrated, the Hybrid BNM is a boundary-only meshless approach. No boundary elements are used for neither interpolation nor integration purposes. Therefore, it can circumvent the discretisation difficulty to a large extent.

4. Numerical Results

In this section we present two application examples of the heat conduction analysis of CNT-based composites. The first example deals with a unit model of RVE containing single CNT, while the second demonstrates simulation involving curved CNT and study the effect of its waviness on thermal properties of composites.

4.1 Heat conduction in a square RVE containing single straight CNT

A unit model of a representative volume element with single nanotube is presented in Fig. 1 (a) with dimensions given in Fig. 1 (b). Figure 1 (c) shows the computational model discretised with boundary nodes. Homogeneous boundary conditions are considered here, namely, uniform temperatures of 300 K and of 200 K imposed at the two end faces of the RVE, respectively, and heat flux free at all other faces of the RVE and the inner face of the CNT cavity. This boundary condition set allows us to estimate equivalent heat conductivity of CNT-based composite in the axial direction. Assuming homogeneous material properties and using Fourier's law, the formula for equivalent heat conductivity can be written as:

$$\kappa = -\frac{qL}{\Delta\phi}, \tag{16}$$

where κ represents the heat conductivity; q is the heat flux density, L the length of the RVE in the axial direction and $\Delta\phi$ the temperature difference between the two end faces.

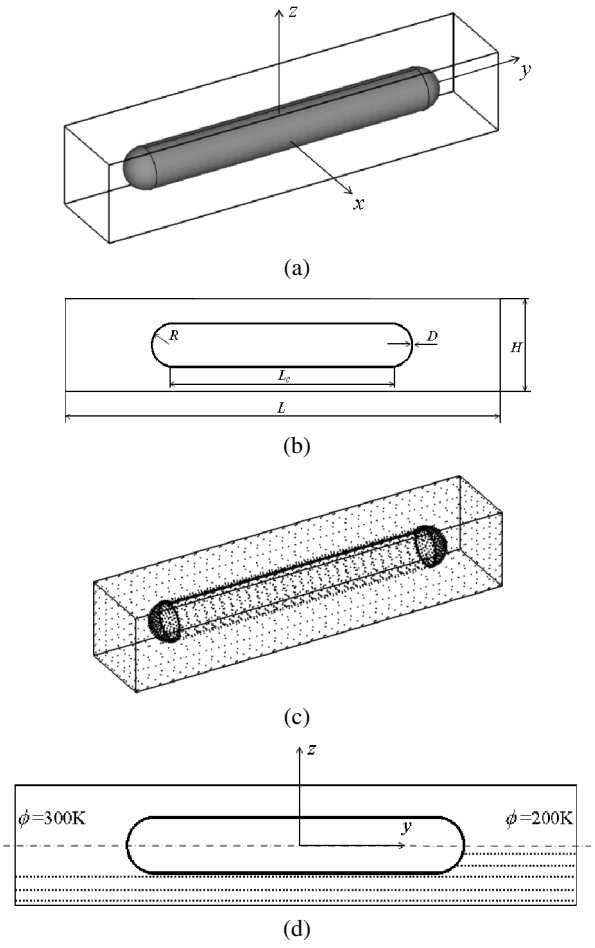

Fig. 1 Nanoscale representative volume element containing a straight nanotube. (a) The unit model and coordinates system; (b) Dimensions of the unit model; (c) Discretisation with boundary nodes; (d) Boundary conditions and results output locations

In the following section, several RVE models for single-walled carbon nanotube of various lengths in a matrix material are studied using the Hybrid BNM, in order to evaluate the equivalent material constant of the CNT-based nanocomposites. The temperature distribution and heat fluxes are computed, and then the equivalent material constants are calculated for the RVEs with CNTs of different lengths.

4.1.1 Temperature distribution and fluxes in a square RVE First, an RVE for a CNT of a specific length is studied. The dimensions of the RVE are: for the matrix, length $L = 100$ nm, $H = 20$ nm; for the CNT, length $L_c = 70$ nm, outer radius $R = 5$ nm, thickness $D = 0.4$ nm (which is close to the theoretical value of 0.34 nm for Single-walled CNT (SWCNT) thickness). The heat conductivities used for the CNT and matrix (polycarbonate) are:

CNT: $\kappa^t = 6\,000\,\mathrm{W/m\cdot K}$;

Matrix: $\kappa^m = 0.19\,\mathrm{W/m\cdot K}$;

These values are within the wide range of dimensions and material constants for CNTs reported in literature[(1)–(11)].

It should be noted here that: (i) the thickness of the CNT is very small; and (ii) the difference of heat conductivity between the CNT and the matrix is extremely large. In this simulation, 2 208 nodes are used for the CNT and 2 192 nodes for the matrix as illustrated in Fig. 1 (c). All calculation results were compared with that obtained using the traditional BEM analysis, and found to be in a good agreement.

The temperature distribution and heat flux in the axial direction (along the dotted lines in Fig. 1 (d)) are presented in Fig. 2 (a) and Fig. 2 (b), respectively. In Fig. 2 (a) it can be seen that the temperature at the CNT cap (fullerence) is uniform and equals to 250 K, from which the temperature decreases to the prescribed value, 200 K, at the end square face of the RVE. Around the CNT cap the heat flux concentration occurs (Fig. 2 (b)). It is noted that the direction of the heat flux density q_y shown in Fig. 2 (b) is in the y-axis direction which is different from the outer normal of the CNT cap. When $z = 0$, q_y equals to the normal flux at the tip point of the cap; while at the edge point of the cap where $z = -5$, q_y is nearly zero, although the normal flux at this point is much higher due to the heat flux concentration.

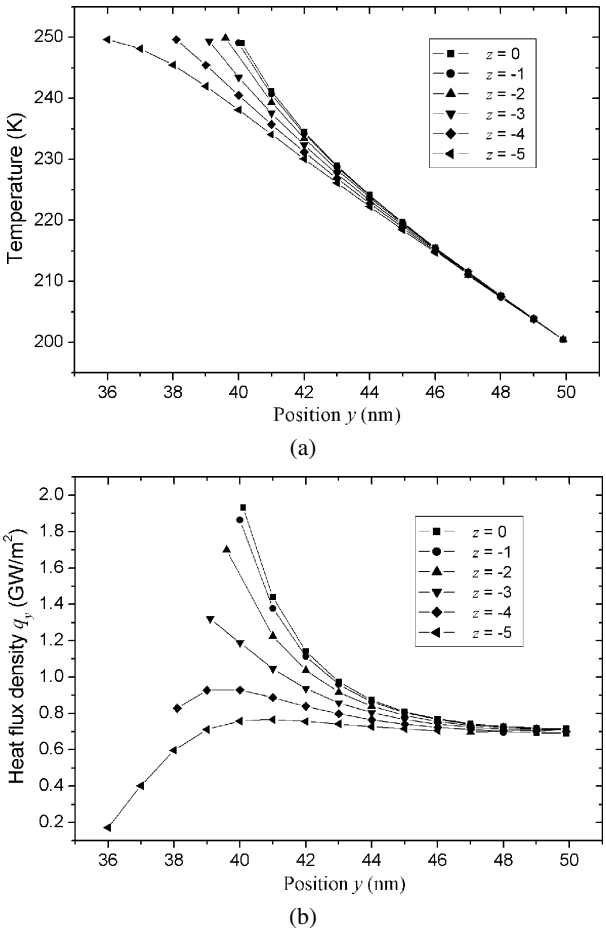

Fig. 2 Temperature and heat flux distribution near the tip cap of the CNT

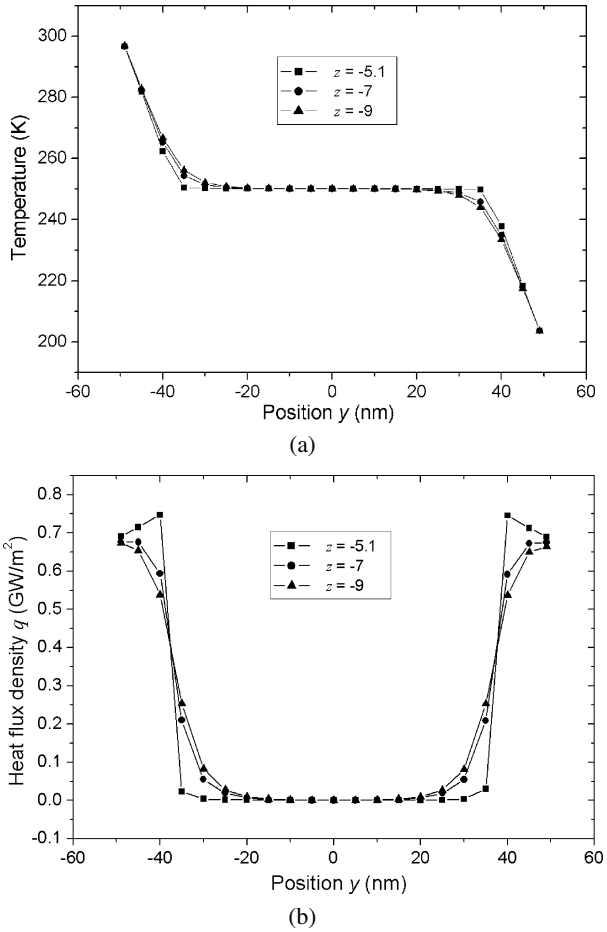

Fig. 3 Temperature and heat flux distribution along the lines through the matrix

Figure 3 presents the temperature and heat flux distribution in the axial direction along the lines through the matrix. An obvious feature of the temperature distribution is observed in Fig. 3 (a) that the temperature in the matrix first decreases from prescribed temperature value at the square end face, then remains almost constant at the segments near the CNT, and finally continues to decrease to the lowest temperature at the other square end face. This observation is consistent with the physical interpretation. Due to that the heat conductivity of the CNT is higher several orders of magnitude over that of the matrix, almost entire flux flows through the CNT. Therefore, nearly no flux flows in the matrix in the segments near the CNT, and the temperature at these locations is almost uniform. The corresponding heat flux concentrations are also observed near the tips of the CNT. The heat fluxes in the matrix along the lines near the CNT are almost zero (see Fig. 3 (b)). The volume fraction of the CNT for this model is 15%, which is calculated using the following equation:

$$v^n = \frac{V^n + V^c}{V^n + V^c + V^p}, \tag{17}$$

where v^n is volume fraction of the nanotube; V^n, V^c and V^p are volumes of the nanotube, the cavity inside the nanotube and the polymer, respectively. The equivalent heat conductivity of this RVE is 0.678 7 W/m·K, which is 3.57 times that of the matrix.

4.1.2 Equivalent constants of composites with various CNT lengths To study the influence of CNT length on the equivalent material constant, several models with various CNT lengths have been considered. In the computations, the dimensions and parameters are that of section 4.1.1, except for the length L_c, which varies from 30 nm to 80 nm. The equivalent heat conductivity of the RVE as a function of L_c is shown in Fig. 4. Results indicate that equivalent heat conductivity is determined mainly by the length of the CNT and the value of the matrix heat conductivity, and relatively less affected by the value of the heat conductivity of the CNT. This may be explained by the fact that the heat conductivity of the CNT is so high, that it can be considered as a super heat conducting material (even if its value is reduced by factor of 10), and the temperature within the CNT can be taken as uniform. Based on this observation, we propose an approximate formula for estimation of equivalent constant in the axial direction as follows:

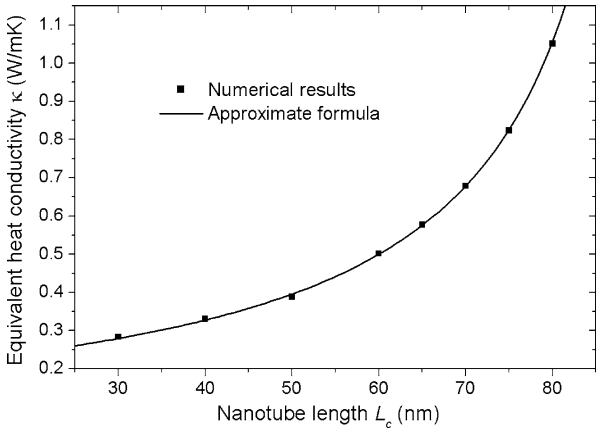

Fig. 4 Equivalent heat conductivity of the RVE for different CNT length

$$\kappa^e = \kappa^m \frac{L}{L - L_c - 0.4R}. \tag{18}$$

In this formula, the CNT serves as a super heat conductor which reduces the distance of the heat conducting path. The equivalent heat conductivities estimated by means of Eq. (18) for various lengths of the CNT are also presented in Fig. 4. It can be seen that the equivalent heat conductivities for CNTs calculated by using Eq. (18) are in a very good agreement with that of numerical simulations. For the cases $L_c = 30$ nm and $L_c = 80$ nm, the volume fractions of the CNTs are 7.2% and 17%, and the equivalent heat conductivities are 1.49 and 4.34 times that of the matrix, respectively.

4.2 Heat conduction in RVE containing curved CNT

In order to study the effect of CNT waviness and its influence on thermal properties of nano-composites, the unit RVE model with the curved CNT embedded is used. The geometry and boundary conditions are presented in Fig. 5 (a) – (c) while Fig. 5 (d) shows the computational model discretised with boundary nodes.

Nanotube waviness is considered by prescribing a sinusoidal NT shape as:

$$z = A \sin\left(\frac{2\pi y}{L_c}\right), \tag{19}$$

where L_c stands for the wave length of the sinusoid function, and y is the fiber axial direction.

Again, homogeneous boundary conditions are applied, namely uniform temperatures of 300 K and of 200 K imposed at the two end faces of the RVE, respectively, and heat flux free at all other faces of the RVE and the inner face of the CNT cavity.

4.2.1 Temperature and fluxes distributions in an RVE with a curved CNT An RVE for a curved CNT of a specific length and waviness is first studied. The dimensions of the RVE are: for the matrix, length L = 100 nm, B = 20 nm and H = 60 nm; for the CNT, length L_c = 70 nm, A = 20 nm outer radius R = 5 nm, thickness

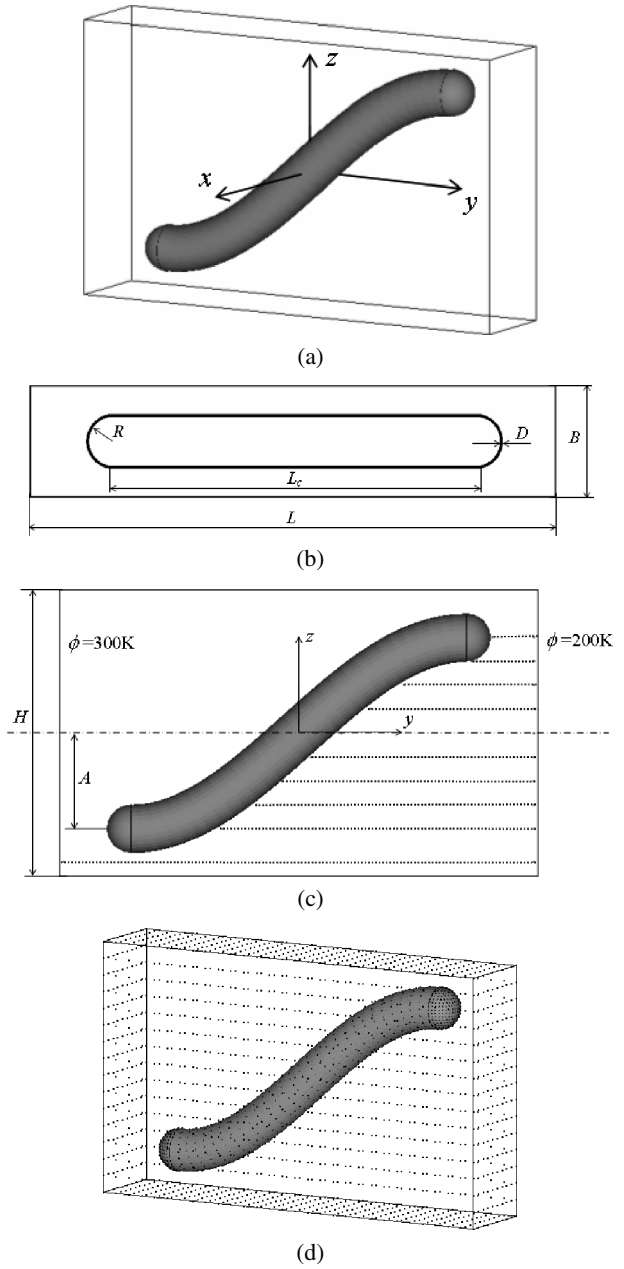

Fig. 5 Nanoscale representative volume element with a curved nanotube embedded. (a) The unit model and coordinates system; (b) Top view: dimensions; (c) Side view: dimensions, boundary conditions and results output locations; (d) Discretisation with boundary nodes

D = 0.4 nm. The heat conductivities used for the CNT and matrix are those of previous section.

Temperature distribution and heat flux in the axial direction are presented in Fig. 6. Again, it is seen (Fig. 6 (a)) that temperatures at the locations close to CNT (the start points for each dotted line except the one that passes all through the matrix) are almost uniform. The corresponding heat flux concentrations are also observed near the tip of the CNT (z = 20) in Fig. 6 (b). The heat fluxes in the matrix at the locations near the middle part of the CNT

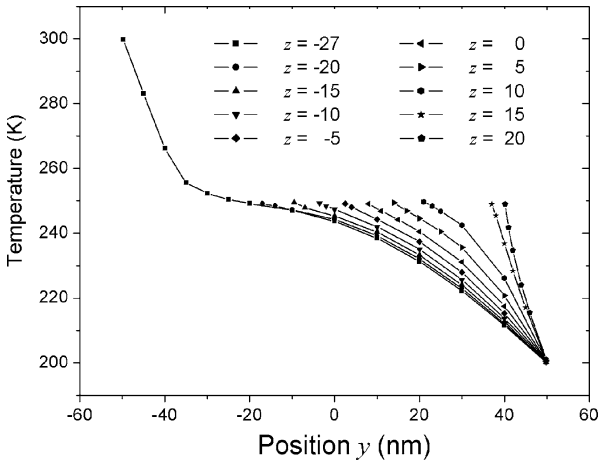

(a)

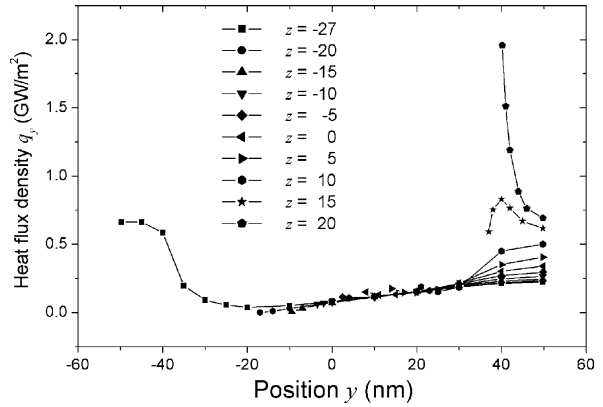

(b)

Fig. 6 Temperature and heat flux distribution in the matrix

are very small and approaching zero.

4. 2. 2 Equivalent constants of composites with various CNT waviness The influence of CNT waviness on the equivalent material constant, employing several models with various CNT waviness ratios, is also investigated. Dimensions and parameters of section 4.2.1 are kept, except for the waviness ratio ($w = A/L_c$) and the ratio of the phase constant ($C_r = \kappa^{\mathrm{CNT}}/\kappa^{\mathrm{matrix}}$). The waviness ratio is changed by varying the amplitude A of the sinusoid curve while keeping the half waviness L_c constant. Computations were performed for the following phase constant ratios: $C_r = 30\,000$, $C_r = 300$ and $C_r = 30$. For each value of C_r the conductivity of the matrix is held constant at 0.19 W/m·K. The equivalent heat conductivity of the RVE as a function of w is presented in Fig. 7. Results demonstrate that equivalent heat conductivity is only slightly dependent on the CNT waviness for both high and low ratios of the phase conductivity. These results are in a sharp contrast to that of the elasticity problem[11], where the equivalent Young's modulus quickly decreases with increasing nanotube curvature.

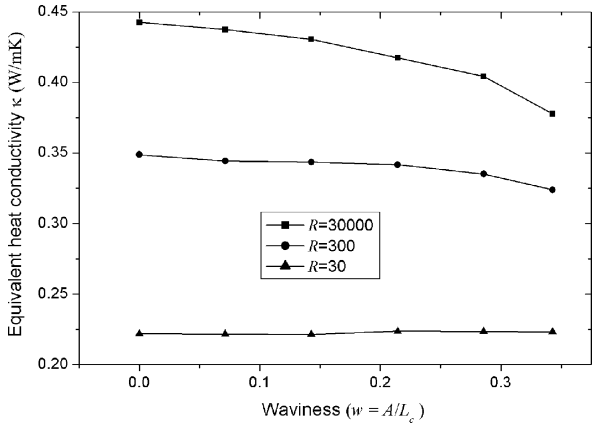

Fig. 7 Equivalent heat conductivity for various waviness

5. Conclusions and Discussion

The paper presents an implementation of Hybrid BNM to the heat conduction analysis in bodies containing thin-walled structures. The Hybrid BNM is a meshless, boundary-only method requiring discrete nodes located on bounding surfaces of the domain of interest, only. Moreover, it uses the parametric representation of those surfaces, and as such representation is employed in any CAD software, commercial packages may be exploited. That greatly simplifies the pre-processing and discretization tasks and makes approach extremely useful, and more cost- and resources-effective than based on conventional FEM/BEM models.

Mathematical models presented in the paper rely on continuum mechanic principles and do not account for quantum effects. However, the continuum-based models seem to be so far the only feasible one for performing preliminary simulations of nano-composites behavior and properties at practical/engineering level. Hence, models and solution procedures outlined in this study may be used for any inclusion problem.

The multi-domain Hybrid BNM formulation presented here may be easily extended and enhanced for problems involving randomly distributed CNTs of various lengths, shapes and orientations, employing the Fast Multipole expansion approach[18),(19)]. This is a subject of ongoing research and will be reported shortly.

At current stage, numerical results demonstrate that temperatures within the CNT and at the interface are almost uniform, and heat flux concentration occurs at the two tips of the CNT. With the addition of CNTs of about 7.2% and 17% (by volume fraction) to the composite, the heat conductivity in the CNT axial direction can increase as many as 49% and 334%. The presented results show that the equivalent heat conductivity is determined mainly by the length of the CNT, and less affected by the value of the CNT heat conductivity. An approximate formula for estimating the equivalent material constant has been

given, which is found to be of reasonable accuracy in estimating the equivalent heat conductivity in the CNT axial direction. The effects of the CNT waviness on the equivalent conductivity were also investigated. In contrast to the elastostatic case[11], the presented results show that the equivalent heat conductivity is less affected by the waviness of the CNT.

Acknowledgements

This work was supported by the CLUSTER of Ministry of Education, Culture, Sports, Science and Technology (Japan). The first author would like to thank Mr. K. Tomokiyo for his help during the course of this research.

References

(1) Endo, M., Kim, Y.A., Nishimura, K., Matushita, T. and Hayashi, T., From Vapor-Grown Carbon Fibers (VGCFs) to Carbon Nanotubes, Carbon Filaments and Nanotubes: Common Origins, Differing Applications, edited by Biro, L.P., Bernardo, C.A., Tibbetts, G.G. and Lambin, P.h., Kluwer Academic Publishers, NATO Science Series E: Applied Sciences, Vol.372 (2001), pp.51–61.

(2) Endo, M., Kim, Y.A., Hayashi, T., Nishimura, K., Matushita, T., Miyashita, K. and Dresselhaus, M.S., Vapor-Grown Carbon Fibers (VGCFs): Basic Properties and Their Battery Applications, Carbon, Vol.39 (2001), pp.1287–1297.

(3) Hone, J., Whitney, M., Piskoti, C. and Zettl, A., Thermal Conductivity of Single-Walled Nanotubes, Phys. Rev. B, Vol.59, No.4 (1999), pp.2514–2516.

(4) Yi, W., Lu, L., Zhang, D.L., Pan, Z.W. and Xie, S.S., Linear Specific Heat of Carbon Nanotubes, Phys. Rev. B, Vol.59 (1999), pp.9015–9018.

(5) Kim, P., Shi, L., Majumdar, A. and McEuen, Pl., Thermal Transport Measurements of Individual Multiwalled Nanotubes, Phys. Rev. Lett., Vol.87, No.21 (2001), pp.215502-1–4.

(6) Berber, S., Kown, Y.-K. and Tomanek, D., Unusually High Thermal Conductivity of Carbon Nanotubes, Phys. Rev. Let., Vol.84, No.20 (2000), pp.4613–4617.

(7) Osman, M.A. and Srivastava, D., Temperature Dependence of the Thermal Conductivity of Single-Wall Carbon Nanotubes, Nanotechnology, Vol.12, No.1 (2001), p.24.

(8) Che, J., Cagin, T. and Goddard, III, W.A., Thermal Conductivity of Carbon Nanotubes, Nanotechnology, Vol.11 (2000), pp.65–69.

(9) Qian, D., Dickey, E.C., Andrews, R. and Rantell, T., Load Transfer and Deformation Mechanisms in Carbon Nanotube Polystyrene Composites, Applied Physics Letters, Vol.76, No.20 (2000), pp.2868–2870.

(10) Liu, Y.J. and Chen, X.L., Evaluations of the Effective Material Properties of Carbon Nanotube-Based Composites Using a Nanoscale Representative Volume Element, Mechanics of Materials, Vol.35 (2003), pp.69–81.

(11) Fisher, F.T., Bradshaw, R.D. and Brinson, L.C., Effects of Nanotube Waviness on the Modulus of Nanotube-Reinforced Polymers, Applied Physics Letters, Vol.80, No.24 (2000), pp.4647–4649.

(12) Hyer, M.W., Stress Analysis of Fiber-Reinforced Composite Materials, (1998), McGraw-Hill, Boston.

(13) Zhang, J.M., Yao, Z.H. and Li, H., A Hybrid Boundary Node Method, International Journal for Numerical Methods in Engineering, Vol.53 (2002), pp.751–763.

(14) Zhang, J.M. and Yao, Z.H., Meshless Regular Hybrid Boundary Node Method, Computer Modeling in Engineering & Sciences, Vol.2 (2001), pp.307–318.

(15) Zhang, J.M., Yao, Z.H. and Tanaka, M., The Meshless Regular Hybrid Boundary Node Method for 2-D Linear Elasticity, Engineering Analysis with Boundary Elements, Vol.27 (2003), pp.259–268.

(16) Zhang, J.M. and Yao, Z.H., Analysis of 2-D Thin Structures by the Meshless Regular Hybrid Boundary Node Method, Acta Mechanica Sinica, Vol.15 (2002), pp.36–44.

(17) Zhang, J.M., Tanaka, M. and Matsumoto, T., Meshless Analysis of Potential Problems in Three Dimensions with the Hybrid Boundary Node Method, International Journal for Numerical Methods in Engineering, Vol.59 (2004), pp.1147–1160.

(18) Greengard, L. and Rokhlin, V., A New Version of the Fast Multipole Method for the Laplace Equation in Three Dimensions, Acta Numerica, Vol.6 (1997), pp.229–269.

(19) Nishida, T. and Hayami, K., Application of the Fast Multipole Method to the 3D BEM Analysis of Electron Guns, edited by Marchettia, M., Brebbia, C.A. and Aliabadi, M.H., Boundary Elements XIX, (1997), pp.613–622, Computational Mechanics Publications.